Pergamon

Geochimica et Cosmochimica Acta, Vol. 68, No. 17, pp. 3521–3530, 2004

0016-7037/04 $30.00 + .00

doi:10.1016/j.gca.2004.02.018

History of carbonate ion concentration over the last 100 million years

Toby Tyrrell[1,*] and Richard E. Zeebe[2,†]

[1]School of Ocean and Earth Science, Southampton Oceanography Centre, Southampton University, Southampton SO14 3ZH UK
[2]Alfred Wegener Institute, Am Handelshafen, D-27570 Bremerhaven Germany

(*Received July* 23, 2003; *accepted in revised form February* 6, 2004)

Abstract—Instead of having been more or less constant, as once assumed, it is now apparent that the major ion chemistry of the oceans has varied substantially over time. For instance, independent lines of evidence suggest that calcium concentration ($[Ca^{2+}]$) has approximately halved and magnesium concentration ($[Mg^{2+}]$) approximately doubled over the last 100 million years. On the other hand, the calcite compensation depth, and hence the $CaCO_3$ saturation, has varied little over the last 100 My as documented in deep sea sediments. We combine these pieces of evidence to develop a proxy for seawater carbonate ion concentration ($[CO_3^{2-}]$) over this period of time. From the calcite saturation state (which is proportional to the product of $[Ca^{2+}]$ times $[CO_3^{2-}]$, but also affected by $[Mg^{2+}]$), we can calculate seawater $[CO_3^{2-}]$. Our results show that $[CO_3^{2-}]$ has nearly quadrupled since the Cretaceous. Furthermore, by combining our $[CO_3^{2-}]$ proxy with other carbonate system proxies, we provide calculations of the entire seawater carbonate system and atmospheric CO_2. Based on this, reconstructed atmospheric CO_2 is relatively low in the Miocene but high in the Eocene. Finally, we make a strong case that seawater pH has increased over the last 100 My. *Copyright © 2004 Elsevier Ltd*

1. INTRODUCTION

1.1. Climate, Atmospheric pCO_2, and Ocean Carbonate Chemistry

The Earth's carbon cycle is currently being subjected to a severe perturbation in the form of burning of long-buried fossil fuels. Understanding the functioning of the historical carbon cycle may help us understand the implications of our present perturbations to it.

There are still many open questions: for instance, although carbon dioxide is strongly suspected to play a major role in controlling climate, there is still much uncertainty, with evidence of warm climates at times of suspected low atmospheric CO_2 (Flower, 1999; Pagani, 1999). The ice core record of atmospheric CO_2 concentrations exists only over the last 400,000 yr or so. We do not have any direct evidence to tell us whether the very warm Cretaceous period (135–65 Mya) was caused by high atmospheric CO_2. While it is suspected that the slow deterioration in Earth climate since the Cretaceous (the trend towards an icehouse Earth; Zachos et al., 2001) has been caused by declining atmospheric CO_2, lack of data prevents a definitive interpretation. More indirect approaches are, therefore, required to reconstruct the long-term history of atmospheric CO_2. One possible approach is by reconstructing the history of carbonate chemistry ($[CO_2(aq)]$, $[HCO_3^{2-}]$, $[CO_3^{2-}]$) of seawater over time. The atmosphere and the surface ocean reach carbon equilibrium within about a year, and significant imbalances cannot be maintained for longer than this. If the history of surface ocean carbonate chemistry can be calculated, then so too can the history of atmospheric CO_2.

1.2. Long Timescale Variations in Ca and Mg Concentrations

In the absence of evidence to the contrary, it was previously assumed that the concentrations of the major ions making up the dissolved salt in seawater (Cl^-, Na^+, SO_4^{2-}, Ca^{2+}, Mg^{2+}, and K^+) were more or less constant over geological timescales (Holland, 1978; Holland, 1984), and more rapid variations are precluded by residence times measured in millions of years (Berner and Berner, 1996). However, recent evidence shows that ocean composition has been far from constant. In this paper, the concern is primarily with calcium and magnesium concentrations. The lines of evidence for slow oscillations in seawater $[Ca^{2+}]$, $[Mg^{2+}]$, and therefore, (Mg/Ca) are as follows:

1. The mineralogy of inorganic (nonskeletal) carbonate cements and ooids has varied over time in the geological record, with predominance of aragonite forms at some times and calcite forms at other times (Sandberg, 1983). Laboratory experiments (e.g., Morse et al., 1997) show that either calcite or aragonite precipitates out first from a solution dependent on its temperature and also on its chemistry, particularly its Mg/Ca ratio. The variation in the form of inorganically precipitated calcium carbonate through time led Sandberg to suggest an alternation in seawater chemistry: between "calcite seas" and "aragonite seas."
2. Hardie (1996) noted that temporal changes in the mineralogy of potash evaporites in the geological record also track Sandberg's curve, with potash deposits characterised by $MgSO_4$ salts more common during aragonite seas, and potash deposits characterised by KCl salts more common during calcite seas.
3. A wide array of evidence (Stanley and Hardie, 1998) suggests that the variation in the nature of biologically precipitated (skeletal) carbonate rocks obeys a similar variation to that of the inorganic cements and ooids. Among fossilised

* Author to whom correspondence should be addressed (t.tyrrell@soc.soton.ac.uk).
† University of Hawaii at Manoa, SOEST, 1000 Pope Road, MSB 504, Honolulu, Hawaii 96822 USA

'hypercalcifying' organisms (corals, sponges, coralline algae, etc.), aragonitic species were more common during Sandberg's aragonite seas, whereas calcitic species were more common during Sandberg's calcite seas.

4. These indirect suggestions of Mg/Ca oscillations have recently been reinforced by more direct measurements, from fluid inclusions in marine halites (e.g., Lowenstein et al., 2001; Horita et al., 2002). These fluid inclusions (microscopic globules trapped in salt crystals as they form in evaporating seawater) contain evidence of the ocean chemistry at that time. The partially evaporated nature of the fluid inclusions excludes a completely straightforward reconstruction of past seawater composition, but much information can still be derived. An immediate point of interest is that the chemistry of the fluid inclusions is often very different from that of any point along the evaporation pathway of modern-day seawater, implying very different pre-evaporation chemistries. It is not possible to evaporate modern day seawater to produce a brine resembling many of the Phanerozoic fluid inclusions. Similarities in chemical composition of fluid inclusions in rocks of similar age, but deposited in different parts of the world, argue for control by swings in global seawater composition rather than by local or regional processes (Lowenstein et al., 2001; Horita et al., 2002). The concentrations of ions unlikely to precipitate out until very late in the evaporation sequence, and with very long residence times in seawater (e.g., Br^-, ~100 My; (Holland, 1978)), can give an idea of the "degree of evaporation" of each inclusion. Two of the earliest salts to precipitate out as seawater becomes progressively more concentrated are calcium carbonate ($CaCO_3$), then gypsum/anhydrite ($CaSO_4$); the presence of residual [Ca^{2+}] but no [SO_4^{2-}] in samples from some times, in contrast to residual [SO_4^{2-}] but no [Ca^{2+}] at other times, points to variations in the initial [Ca^{2+}] and [SO_4^{2-}]. Through the use of these and other techniques and assumptions, best-guess [Ca^{2+}] and [Mg^{2+}] concentrations (Zimmermann, 2000; Horita et al., 2002) and seawater (Mg/Ca) (Lowenstein et al., 2001; Horita et al., 2002) have been calculated back through time from the fluid inclusions, and they agree well with Sandberg's calcite and aragonite seas.
5. Another recent record for past seawater (Mg/Ca) has been obtained from the (Mg/Ca) of echinoderm skeletons (Dickson, 2002). Echinoderms incorporate Mg and Ca into their shells in a variable ratio linked to that of the seawater they grow in. Their fossilized skeletons have been analysed and the inferred history of Mg/Ca broadly supports that from fluid inclusions (Dickson, 2002).
6. Stanley et al. (2002) found in laboratory culture experiments that, like echinoderms, the (Mg/Ca) of the calcite skeletons of coralline algae reflects that of the seawater medium they grow in. The predominance of low-Mg calcite fossils during calcite seas (low seawater Mg/Ca), and of high-Mg calcite fossils during aragonite seas, (high seawater Mg/Ca) (Stanley and Hardie, 1998) therefore, also supports variable seawater (Mg/Ca) through time.

Considering only the last 100 My, the cause of the changes is uncertain, but may involve long-term variations in midocean ridge spreading rates (Hardie (1996); but see also Holland et al. (1996) and Holland and Zimmermann (1998) for counterarguments), or alternatively, a change in the mode of calcium carbonate deposition (Volk, 1989). The timing of the beginning of the most recent seawater calcium decline corresponds approximately with the laying down of the first massive coccolith chalks in the Late Cretaceous (99–65 Mya) and the beginning of significant calcium carbonate flux to deep ocean sediments following the rise to abundance of the main planktonic calcifiers, coccolithophores and foraminifera (Volk, 1989; Hay, 1999). Most shelf sediments are eventually uplifted and the calcium within them then returned by erosion to rivers and then back to the sea; most deep-sea sediments, in contrast, are eventually subducted at continental margins, taking calcium down into the mantle. Increasing Ca^{2+} loss from the oceans has been accompanied by decreasing Mg^{2+} loss, probably because dolomitisation (formation of $CaMg(CO_3)_2$ rocks) is thought to have only taken place in shallow environments (Holland and Zimmerman, 2000).

Regardless of the cause, the point of interest for this paper is that, taken as a whole, "these studies develop an argument of unprecedented strength for a chemically dynamic ocean over the past half billion years of Earth history" (Montanez, 2002), in particular for [Ca^{2+}] and [Mg^{2+}]. The combined evidence (Fig. 1) suggests that [Ca^{2+}] was more than 100% higher 100 Mya than it is today, whereas [Mg^{2+}] was somewhere near half of today's value.

1.3. Implications for Dissolution of Calcium Carbonate in Seawater

The long-term progressive fall in seawater calcium concentration must have affected the ocean carbon system. Calcification and dissolution in the ocean have been shown to be sensitive to the calcite or aragonite saturation state of seawater (Ω), which is defined as

$$\Omega = [Ca^{2+}] \cdot [CO_3^{2-}]/K_{sp} \quad (1)$$

where K_{sp} is the stoichiometric solubility product (different for aragonite or calcite), which varies in present-day surface waters primarily as a function of temperature and salinity (Mucci, 1983). The incorporation of some magnesium rather than calcium ions into the crystal lattice affects the solubility of calcite, and we account for this effect of [Mg^{2+}] on K_{sp} (section 2.2). Expressing the equation in terms of concentrations rather than activities is acceptable for our purposes (section 2.3).

Taking [Ca^{2+}] and [Mg^{2+}] from Figure 1 and assuming all else (including [CO_3^{2-}]) at present-day values, then Ω at 100 Mya would have been ~threefold higher than today. This would produce a CCD at ~10 km depth (Eqn. 4 of Jansen et al. (2002)), that is to say, preventing any dissolution of $CaCO_3$ in the ocean. A 10 km deep CCD is unlikely given the process of carbonate compensation which exerts negative feedback on a timescale of ~10,000 yr (Sundquist, 1990; Sigman et al., 1998); in any case it is ruled out by the geological data.

1.4. Near-Constancy of Calcium Carbonate Saturation State During the Last 100 Million Years

To our knowledge there are four sources of information about the history of the calcium carbonate saturation state of the ocean:

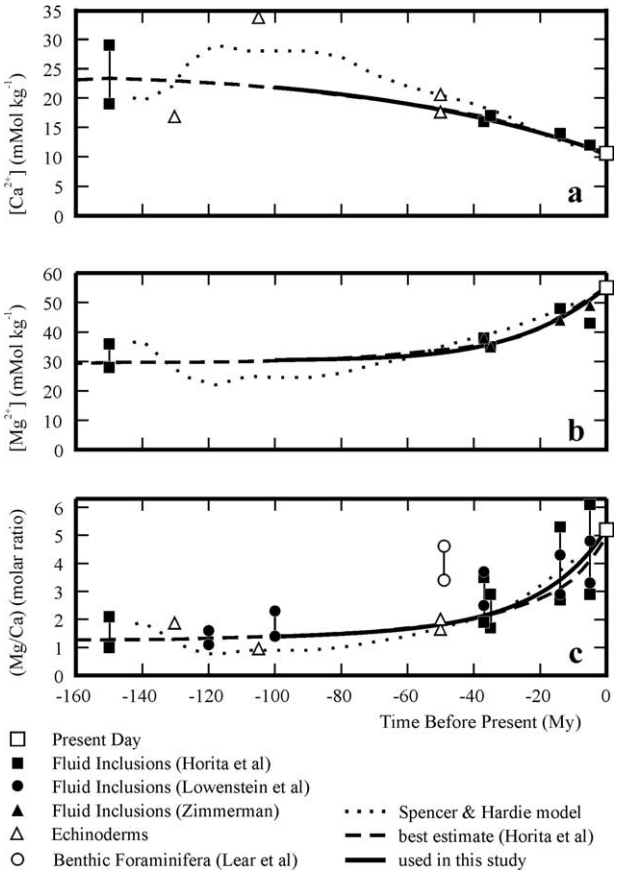

Fig. 1. Seawater composition over the last 160 million years: (a) calcium ion concentration (mMol kg^{-1}); (b) magnesium ion concentration (mMol kg^{-1}); and (c) magnesium/calcium ratio (Mol/Mol). (■, ●, ▲) from fluid inclusions in evaporites (Horita et al., 2002; Lowenstein et al., 2001; and Zimmermann, 2000; respectively), with parent seawater calculated from the composition of partially evaporated brine trapped in salt crystals. (Δ) (Mg/Ca) from fossil echinoderms (Dickson, 2002), or, in the case of $[Ca^{2+}]$, calculated from fluid inclusion $[Mg^{2+}]$ divided by echinoderm (Mg/Ca); (○) (Mg/Ca) 49 Mya from benthic foraminiferal calcite (Lear et al., 2002); (□) present-day composition of seawater; (dotted line) history of seawater composition according to a model (Spencer and Hardie, 1990; (dashed line) best estimate of past seawater composition according to Horita et al. (2002); (thick line) values used here (0–100 Mya), chosen to agree with best estimate of Horita et al. (2002). A vertical line between two symbols indicates a range of values.

(A) From the history of calcite compensation depth (CCD) in the oceans (Fig. 2). The CCD defines the 'snow line' above which calcium carbonate accumulates on the seafloor, below which it dissolves. The deepest ocean sediments recovered by drilling are calcium carbonate-free at all times during the last 100 My. The 0 to 100 Mya CCD record derived from deep ocean cores (Fig. 2) suggests that, although there has been variability (for instance, Hay, 1988; Lyle, 2003) and a long-term trend to deeper values, nevertheless the ocean average CCD has not varied by more than ~1.5 kilometres from its current value of ~4.8 km. The CCD data imply that Ω has been fairly constant since the Cretaceous despite the concomitant decrease in $[Ca^{2+}]$.

(B) From the abundance of calcifying cyanobacteria (stromatolites) in the fossil record (Arp et al., 2001). These require surface water calcite saturation states ≥10 as a prerequisite for their formation. The geological record contains frequent occurrences of calcifying cyanobacteria throughout most of the Phanerozoic, with the striking exception of the last 100 My, from which time almost no fossilised calcifying cynaobacteria have been found (Arp et al., 2001). One possible interpretation is generally high saturation states through the Phanerozoic, falling to consistently lower values during the last 100 My.

(C) From analysis of the paleolatitudinal ranges of shallow-water biogenic carbonate (Fig. 7B) of Opdyke and Wilkinson (1993)).

(D) From analysis of the paleolatitudinal ranges of inorganically precipitated ooids and cements (Figs. 3 and 4 of Opdyke and Wilkinson (1990)). Neither of these two ranges show large contractions or expansions in the past, such as might be expected to accompany any large shift in average surface ocean Ω.

We take our lead in this paper from the CCD record because of the large number of ocean cores that have been drilled and because of the unmistakable appearance of a CCD shallowing or deepening through a core location (colour change of the core). We use a smoothed fit to the long-term trends in CCD (Fig. 2), which averages out short-term CCD variations such as during the last 20 My (e.g., Lyle, 2003), during temporary episodes such as the Paleocene-Eocene Thermal Maximum (PETM) (Thomas, 1998), and during glacial-interglacial cycles (Barker and Elderfield, 2002). The CCD records deep ocean saturation state. We assume that surface saturation state tracks deep saturation state, but also explore sensitivity to this assumption in the Appendix.

The partitioning of the $CaCO_3$ flux between shallow and deep seas can be an important control on ocean carbonate chemistry, and therefore atmospheric pCO_2 (Opdyke and Wilkinson 1989; Kump and Arthur, 1997). In the GEOCARB model (Berner, 1994; Berner and Kothavala, 2001), atmospheric CO_2 during the last 100 My was found to be quite sensitive to this partitioning (Fig. 11 of Berner (1994)). Large-scale $CaCO_3$ deposition in shallow seas during the Late Cretaceous has been succeeded by increasing importance of deep-sea $CaCO_3$ deposition through the Cenozoic (Hay, 1999). This study, however, is a reconstruction of $[CO_3^{2-}]$ and atmospheric pCO_2 from data. It is not a mechanistic model. The location and processes of $CaCO_3$ burial are, therefore, irrelevant to our purpose except as possible explanations of the reconstructions obtained.

Respiration of organic carbon in sediments can lead to a partial decoupling between deep ocean chemistry and the CCD (Archer and Maier-Reimer, 1994). However, this effect is likely to be of minor importance to this study (see discussion in section 4.5 of Zeebe and Westbroek (2003)). The near-constancy of the differential between planktic and benthic $\delta^{13}C$ (Broecker and Peng, 1998) suggests that the organic carbon fluxes of today are similar to those of the past. The respiration effect is not included in our calculations.

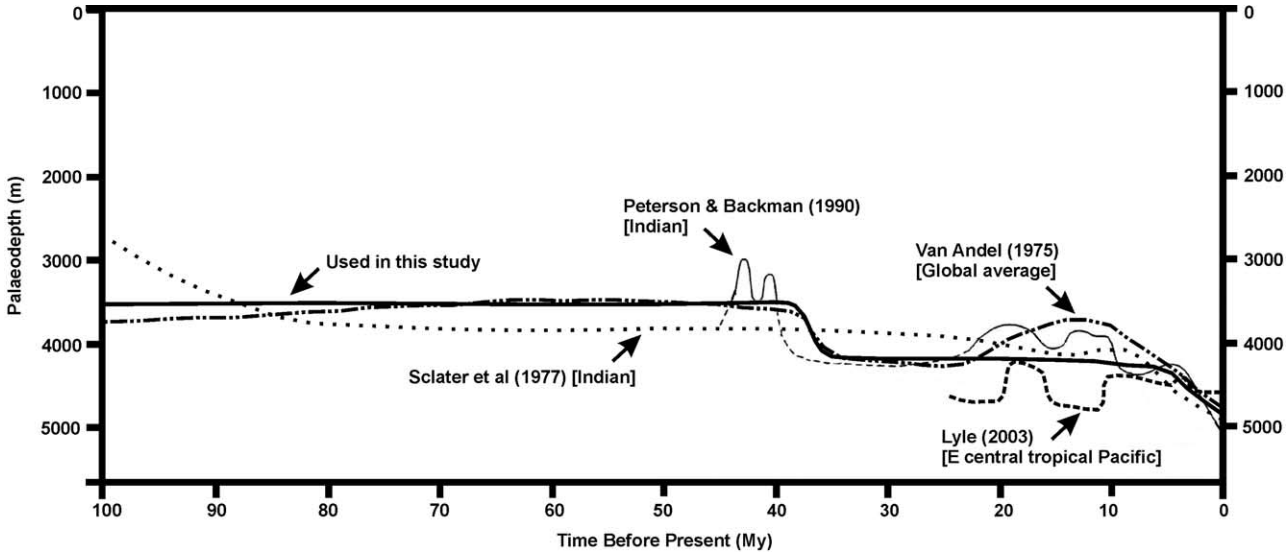

Fig. 2. History of calcite compensation depth (CCD) over the last 100 million years. The solid and dotted lines show reconstructions from core data from the Indian Ocean (Peterson and Backman, 1990; Sclater et al., 1977). The dashed line shows a fit to core data from the eastern central equatorial Pacific (Lyle, 2003). The stippled line shows an estimate of the global average CCD (data from all ocean basins) (van Andel, 1975). The bold line shows the CCD history used here.

2. METHODS

Given the evidence against a large decrease in Ω over time, we reconstruct a best estimate of the evolution of $[CO_3^{2-}]$ over the last 100 My, by assuming nearly constant Ω (Fig. 2) in the face of the changes to $[Ca^{2+}]$ (22 down to 10.6 mMol kg^{-1}) and $[Mg^{2+}]$ (30 up to 55 mMol kg^{-1}) shown in Figure 1.

2.1. Sensitivity to Past Temperature and Salinity

The effects on K_{sp} of possible past variations in temperature and salinity were found to be of minor importance to our results. Past salinity was estimated by forcing it from a reconstruction based on evaporite abundance through time (Hay et al., 2001). This gave similar results to an assumption of constant salinity.

Past global average surface seawater temperature was estimated using the $\delta^{18}O$ record in benthic foraminiferal calcite (Zachos et al., 2001). The record was extended back beyond 65 Mya (into the Cretaceous) using Figure 3 in Wilson et al. (2002) as a guide. A rough correction for the presence of ice sheets was made by assuming that only half of any $\delta^{18}O$ excess above 2‰ is attributable to a temperature effect. Deep-sea temperature derived in this way from benthic foram $\delta^{18}O$ is assumed to be representative of high latitudes where deep water currently forms. Similar temperature changes are assumed to have taken place in tropical waters but with a reduced amplitude of variation (increasing only from 27.5 to 30°C over 100 My). Global average surface temperature (current value 15°C) was then calculated using a quadratic fit to the latitudinal temperature gradient. Due to uncertainties in this and other reconstructions of past temperature, we examined sensitivity of our $[CO_3^{2-}]$ reconstruction to different proposed temperature histories. We used two alternative temperature reconstructions in addition to that just described: (1) from $\delta^{18}O$ in calcitic and aragonitic shells from the photic zone of tropical waters (Veizer et al., 2000), and (2) calculated by pCO_2 of the GEOCARB-III model (Berner and Kothavala, 2001). The maximum difference at any time between $[CO_3^{2-}]$ calculated using two different temperature reconstructions was <1 μMol kg^{-1}. The effect on calculated pCO_2 was larger ($\sim$10%).

2.2. Effect of Mg Concentration on K_{sp} and Dissociation Constants

Calcite saturation state is affected by $[Mg^{2+}]$ as well as $[Ca^{2+}]$, through K_{sp}. We used the relationship $K_{sp}(t) = K_{sp}(0) - \alpha[5.14 - x(t)]$ to calculate K_{sp} at various Mg concentrations, where $K_{sp}(0)$ is today's solubility product of calcite, x(t) is the Mg/Ca ratio of seawater over time, and $\alpha = 3.655 \times 10^{-8}$ (derived from Mucci and Morse (1984)). As a result, K_{sp} increased by $\sim$35% when the seawater Mg/Ca ratio rose (Fig. 1) from 1.4 (100 My) to 5.1 (today).

The effect of $[Mg^{2+}]$ and $[Ca^{2+}]$ on the first and second dissociation constants of carbonic acid (required for calculating the whole carbonate system from any two parameters), K_1 and K_2, was calculated using published sensitivity parameters (Ben-Yaakov and Goldhaber, 1973). For example, a twofold increase of Mg leads to an increase of K_2 by $\sim$28% (equivalent to a shift of pK_2 by about -0.1 units).

2.3. Free Activities and Ion Pairing

Saturation state is properly calculated in terms of activities rather than concentrations, but our use of concentrations is justifiable in this context. Salinity has a fairly small effect on the activities of constant concentrations of calcium and carbonate, for instance, the two activities decrease by $\sim$1 and 4%, respectively, when salinity increases from 35 to 40 (Millero and Schreiber, 1982). Variations in the composition of salinity can also potentially affect activities. Most carbonate ions in seawater are complexed with Mg ions, and we include the effect of varying Mg ion concentration on carbonate ion activity via its effect on the solubility of calcite (section 2.2). Approximately 90% of calcium ions in seawater today exist as free ions (Millero and Schreiber, 1982). This percentage could have been higher in the past due to less abundant SO_4 (Horita et al., 2002), leading to a maximum effect of +10% on calcium activity in the past. Again, this is small compared to changes of >100% in calcium concentration over the last 100Ma.

3. RESULTS

3.1. Carbonate Ion Concentration ($[CO_3^{2-}]$)

Combining the 'best-fit' scenarios (Horita et al., 2002) for $[Ca^{2+}]$ (22 down to 10.6 mMol kg^{-1}) and $[Mg^{2+}]$ (30 up to 55 mMol kg^{-1}) with near-constant calcite saturation state derived from Figure 2 and Eqn. 4 of Jansen et al. (2002), we calculate that surface ocean $[CO_3^{2-}]$ rose by approximately fourfold, from $\sim$55 μMol kg^{-1} at 100 Mya to its present-day value of $\sim$200 μMol kg^{-1} (Fig. 3a). The near-constant CCD docu-

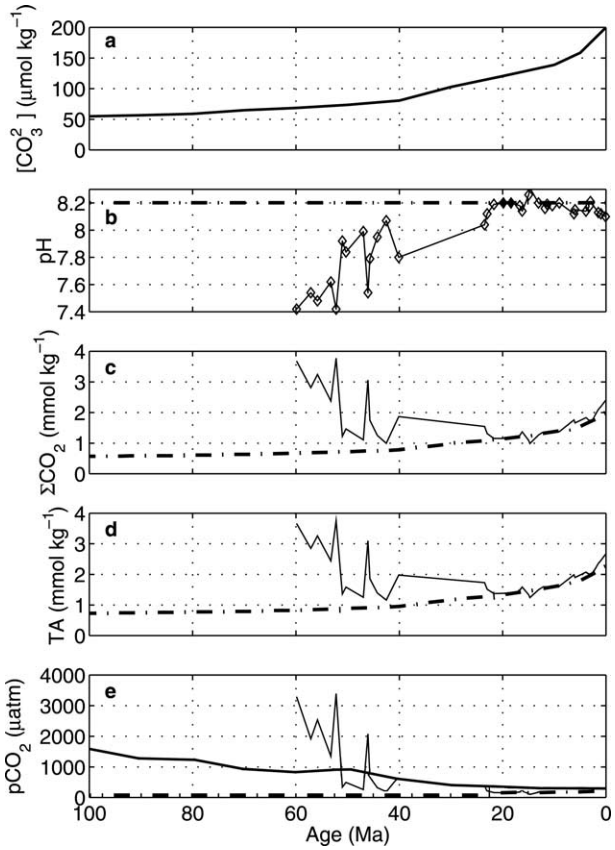

Fig. 3. Reconstruction of CO_2 chemistry of surface seawater: (a) carbonate ion concentration $[CO_3^{2-}]$ (μMol kg^{-1}), from $[Ca^{2+}]$ and $[Mg^{2+}]$ of Figure 1 and saturation state Ω of Figure 2; (b) pH (total pH scale) from the reconstruction of Pearson and Palmer (2000) (solid line), and from constant pH of Lemarchand et al. (2000) (dot-dashed line); (c) ΣCO_2 (sum of all dissolved inorganic carbon, mMol kg^{-1}); (d) total alkalinity (mEquiv, kg^{-1}); and (e) atmospheric pCO_2 (calculated in equilibrium with surface seawater pCO_2, μatm) from (1) variable pH of Pearson and Palmer (2000) and $[CO_3^{2-}]$ (thin line), (2) constant pH = 8.2 and $[CO_3^{2-}]$ (dot-dashed line), and (3) from the GEOCARB-III model (Berner and Kothavala, 2001) (thick line). (c)-(e) are calculated from (a) and (b).

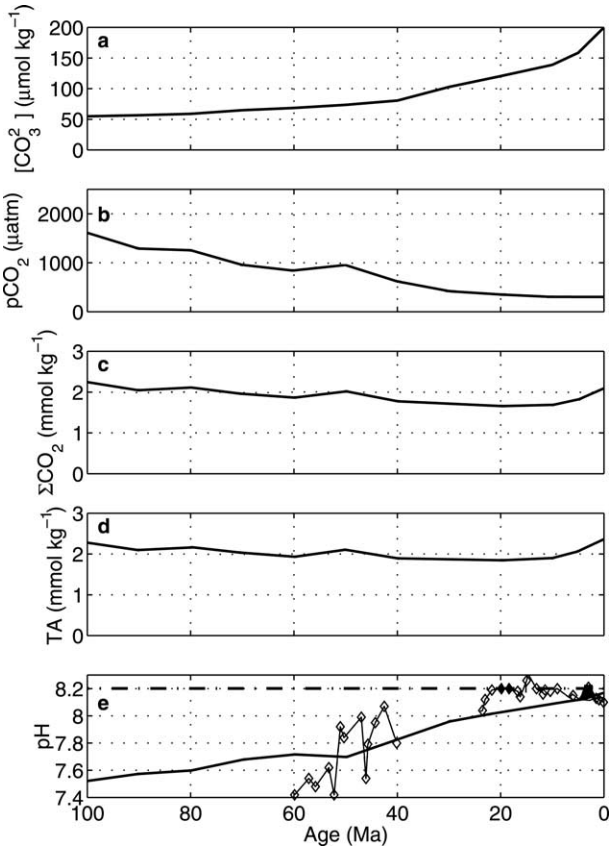

Fig. 4. Reconstruction of CO_2 chemistry of surface seawater: (a) carbonate ion concentration $[CO_3^{2-}]$ (μMol kg^{-1}), from $[Ca^{2+}]$ and $[Mg^{2+}]$ of Figure 1 and saturation state Ω of Figure 2; (b) atmospheric pCO_2 from the GEOCARB-III model (Berner and Kothavala, 2001) (μatm); (c) ΣCO_2 (sum of all dissolved inorganic carbon, mMol kg^{-1}); (d) total alkalinity (mEquiv, kg^{-1}); and (e) pH (total pH scale) calculated from pCO_2 and $[CO_3^{2-}]$ (thick line), from the reconstruction of Pearson and Palmer (2000) (thin line and symbols), and from constant pH (Lemarchand et al., 2000) (dot-dashed line). (c)-(e) are calculated from (a) and (b).

mented in marine sediments records deep-water saturation state, but our reconstruction is of surface-water $[CO_3^{2-}]$. There is, therefore, a potential for our reconstruction to be inaccurate if there have been significant changes over time in the difference between surface and deep water saturation state, for instance, because of changes in the vertical gradients in alkalinity or total dissolved inorganic carbon (DIC). The Appendix contains a discussion of reasons why such gradients probably remained more or less constant over time, but also calculations of sensitivity of our results to possible changes in those gradients over time.

3.2. Atmospheric CO_2 from $[CO_3^{2-}]$ and pH

We now use equations of seawater carbon chemistry (Zeebe and Wolf-Gladrow, 2001) to estimate the implications of changing surface ocean $[CO_3^{2-}]$ on the rest of the carbonate system over the last 100 My. We use dissociation constants for seawater (Lueker et al., 2000) recommended by Prieto and Millero (2002). The impact of varying $[Mg^{2+}]$ on the calculation of carbonate chemistry parameters is also taken into account (section 2.2).

Because the ocean carbonate system ($[CO_2(aq)]$, $[HCO_3^-]$, $[CO_3^{2-}]$, ΣCO_2, alkalinity, pCO_2, and pH) has two degrees of freedom, past atmospheric CO_2 cannot be calculated directly from past $[CO_3^{2-}]$. The whole carbonate system can be calculated from any two parameters, but not from just one.

Past ocean pH has been estimated from the isotopic record of boron assimilated into foraminifera shells (Pearson and Palmer, 1999; Pearson and Palmer, 2000). This was combined with an assumption of constant ΣCO_2 to reconstruct past atmospheric pCO_2 (Pearson and Palmer, 1999). Sundquist (1999) pointed out that the assumption of constant past ΣCO_2 was questionable, and Caldeira and Berner (1999) suggested that pH should be combined instead with an assumption of constant past $[CO_3^{2-}]$, while recognising that this depended on $[Ca^{2+}]$ not varying. In a later paper, atmospheric pCO_2 was calculated from combining pH with an assumption that $[Ca^{2+}]$ has remained proportional to alkalinity (Pearson and Palmer, 2000).

Here we take advantage of the recent work on $[Ca^{2+}]$ and $[Mg^{2+}]$ to reconstruct atmospheric pCO_2 from reconstructions of $[CO_3^{2-}]$ and pH. It is now possible, for the first time, to calculate atmospheric pCO_2 from two independent evidence-based reconstructions of separate carbonate system parameters ($[CO_3^{2-}]$ and pH), with the results shown in Figure 3. In section 4.1 we compare our results to a recent similar study (Demicco et al., 2003).

Our calculation yields low pCO_2 (<280 ppm, the interglacial value) during almost all of the Miocene. In contrast, the calculated pCO_2 is very high during the Eocene, higher than from some other pCO_2 reconstructions (Royer et al., (2001) and references therein), and higher than from the GEOCARB-III model (Berner and Kothavala, 2001).

3.3. pH from $[CO_3^{2-}]$ and Atmospheric CO_2

When the analysis is inverted and pH is calculated from $[CO_3^{2-}]$ and pCO_2 (from the GEOCARB-III model, Berner and Kothavala, 2001), this yields a pH trend over the last 60 My (Fig. 4) which is generally similar in sign to the $\delta^{11}B$-estimated pH, but in which the magnitude of the rise in pH over the whole period is only about half as great (~0.5 U).

4. DISCUSSION

4.1. First Multimillion Year Reconstruction of Carbonate Ion Concentration

Although foraminifera shell thickness has been developed as a proxy for carbonate ion over relatively short timescales (0–0.05 Mya; Barker and Elderfield, 2002), there are, however, no previous reconstructions over timescales longer than a million years. The Berner, Lasaga and Garrels (BLAG) model contained variable $[Ca^{2+}]$, $[Mg^{2+}]$, and $[HCO_3^-]$ (Figs. 9 and 10 of Berner et al. (1983)); but it was not possible at that time to constrain their time histories with data, and they do not resemble those presented here. The development of $[Ca^{2+}]$ and $[Mg^{2+}]$ histories now makes it possible, for the first time, to generate a long-term (100 My) evidence-based reconstruction of carbonate ion concentration (Fig. 3a).

Our reconstruction was developed independently of that of Demicco et al. (2003). They also use calcium, magnesium, and saturation state to reconstruct $[CO_3^{2-}]$ and thence atmospheric CO_2, but they make different, arbitrary, assumptions about the history of calcite saturation state. They assume that the solubility product $[Ca^{2+}][CO_3^{2-}]$ was one-third or two-thirds lower than the modern value during the period 40 to 60 Mya, but was identical to present-day during the last 40 My. In contrast, we derive our history of saturation state from the CCD record shown in Figure 2. We calculate that $[CO_3^{2-}]$ was not less than one-third of today's value between 40 to 60 Mya, whereas Demicco et al. (2003) calculate that it may have been as much as sixfold lower.

We note that Demicco et al. (2003) derive surprisingly low atmospheric CO_2 concentrations between 40 to 52 Mya, including as low as 100 ppm, much lower than preindustrial (~280 ppm) and glacial (~200 ppm) concentrations, and even lower than their reconstructed Miocene values. This is in spite of evidence suggesting warmer climates and the absence of large ice sheets at that time (Zachos et al., 2001); also, other proxies do not predict such low atmospheric CO_2 concentrations at that time (Royer et al., 2001). The period of Demicco et al.'s (2003) surprisingly low atmospheric CO_2 falls within the period during which they make arbitrary assumptions about calcite saturation state.

Although we use the same pH values, we derive atmospheric CO_2 concentrations that are generally higher (minimum values between 40 to 52 Mya of ~200 to 300 ppm). Their low values are a direct consequence of their assumption that the solubility product was only two times the equilibrium value for calcite during that period of time. Moreover, between 52 to 60 Mya, our pCO2 estimates are ~1500 to 3000 ppm, while the reconstruction of Demicco et al. (2003) includes values lower than 500 ppm. We believe that our $[CO_3^{2-}]$ reconstruction is to be preferred because it is derived from the known history of the CCD. Of course, neither the approach of Demicco et al. (2003) nor our own approach, resolves uncertainties in the atmospheric CO_2 reconstruction that arise from the stable boron isotope method of estimating pH.

Uncertainties in the precise values of $[Ca^{2+}]$, $[Mg^{2+}]$, and Ω through time, in part because of sparse data, lead to uncertainties in the details of our reconstruction of $[CO_3^{2-}]$. However, we are confident that the overall sign and the approximate magnitude of change in our reconstruction are correct. This reconstruction of $[CO_3^{2-}]$ represents, we believe, a major contribution to efforts to reconstruct the history of the seawater carbonate system and interlinked atmospheric pCO_2 since the mid Cretaceous. When a consensus view emerges as to the evolution of the carbon cycle over the last 100 My, then we suggest that it will have to include—as an essential prediction—that surface $[CO_3^{2-}]$ underwent a slow rise from ~55 μMol kg^{-1} at 100 Mya to ~200 μMol kg^{-1} today.

Because all parameters of the carbonate system can be calculated from any two, the development of proxies for multiple parameters (e.g., $[CO_3^{2-}]$, pH, $[CO_2(aq)]/pCO_2$) allows checking for consistency. By calculating a third parameter from two independently estimated ones (e.g., sections 3.2 and 3.3), the intercompatibility of different reconstructions can be tested. If, at some time in the future, all reconstructed parameters are consistent, then there can be more confidence that all are accurate.

4.2. Possible Tests

The conclusions of this paper can be tested by further fluid inclusion work, including planned analyses of inclusions of unaltered seawater in marine carbonates (Horita et al., 2002). The U/Ca ratio in fossil corals also holds promise as a test of our projected $[CO_3^{2-}]$ and $[Ca^{2+}]$ history of seawater (pgs 311–313 of Broecker and Peng (1982)). Corals are thought to faithfully incorporate uranium and calcium into their skeletons at nearly the same ratio as they occur in seawater (with little fractionation), and the uranium concentration of seawater may be tied to the carbonate ion concentration (pgs. 311–313 of Broecker and Peng (1982)). If fossil corals are good recorders of seawater ($[CO_3^{2-}]/[Ca^{2+}]$) then we predict that (U/Ca) of corals from 100 Mya will be found to be somewhere close to 13% [= 100% * (55/22)/(200/10.6)] of modern values; in other words, an almost eightfold reduction in the ratio compared to today.

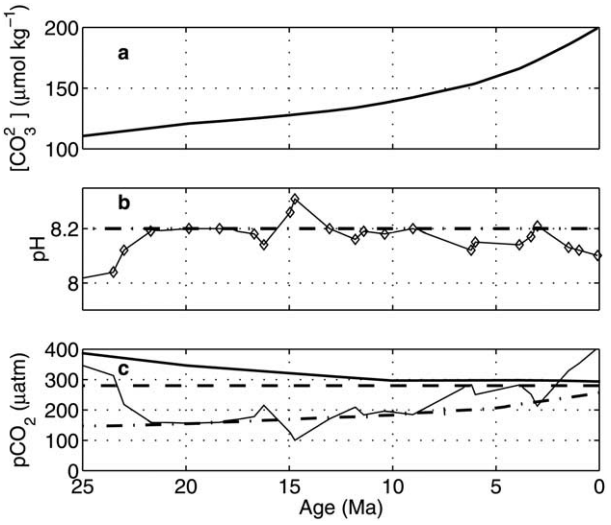

Fig. 5. Carbon chemistry reconstruction during the Miocene only. Shaded area is the Miocene Climatic Optimum (~14.5–17 Mya). Same units and descriptions as in Figure 3, but note different axis scale for pCO_2. Dashed line in (c) shows the preindustrial (Holocene) atmospheric pCO_2, stippled line shows pCO_2 calculated from $[CO_3^{2-}]$ and constant pH of 8.2.

4.3. Mismatch Between Atmospheric CO_2 and Temperature during the Miocene Climatic Optimum?

During the warm Miocene Climatic Optimum (~14.5–17 Mya), fossil floral and faunal evidence indicates climate to have been up to 6°C warmer at this time than at present (Flower, 1999). However, atmospheric pCO_2 similar or lower than today has also been calculated for this time from isotopic fractionation of $C_{37:2}$ alkenones in marine sediments (Pagani et al., 1999). This gives rise to the possibility of warmth without high pCO_2. Some other proxies also indicate pCO_2 only slightly higher than present (Royer et al., 2001).

When we combine our carbonate ion concentration (~130 μMol kg^{-1} during this interval, Fig. 5a) with either constant pH (Lemarchand et al., 2000) or variable pH (Pearson and Palmer, 2000), lower-than-present atmospheric pCO_2 results for both cases (Fig. 5c). Our carbonate ion reconstruction, therefore, supports low atmospheric pCO_2 during this warm period, unless surface ocean pH was lower than present, i.e., opposite in sign to the reconstruction of Pearson and Palmer (2000).

4.4. Increasing pH Over the Last 100 My

The high Eocene pCO_2's are mainly driven by low pH's before 40 Mya (Fig. 3). The much lower ocean pH's 40 to 60 Mya have been questioned by Lemarchand et al. (2000), who came to the contrasting conclusion that pH was maintained "at a roughly constant value on geological timescales." In Figure 3e we have also plotted atmospheric pCO_2 calculated from our $[CO_3^{2-}]$ and from constant pH of 8.2. This leads to pCO_2 of ~90 μatm at 60 Mya, in significant disagreement with other atmospheric pCO_2 reconstructions that all estimate higher-than-present pCO_2 at 50 to 60 Mya (Royer et al., 2001). It, therefore, seems highly unlikely that pH has been nearly constant over the last 60 My. It is much more probable, we believe, that surface ocean pH has increased over the last 100 My.

5. CONCLUSIONS

The first 100 million year-long reconstruction of carbonate ion concentration is presented here, derived from fluid inclusion evidence of variable major ion concentrations and from ocean drilling evidence of saturation state. It gives new insight into the evolution of the oceanic carbonate system over the last 100 My. It provides a strong constraint on the global carbon cycle and atmospheric CO_2 against which future data and models can be tested.

Acknowledgments—We are grateful to Eric Sundquist, Paul Wilson, Martin Palmer, Dieter Wolf-Gladrow, Howard Spero, and Bradley Opdyke for comments and stimulating discussions. We also thank Robert Berner, Juske Horita, and Klaus Wallmann for sending model results and preprints, and Tony Dickson for data. T.T. has benefitted from UK Natural Environment Research Council (GT5/98/15/MSTB) and SOC Research Fellowships.

Associate editor: L. R. Kump

REFERENCES

Arp G., Reimer A., and Reitner J. (2001) Photosynthesis-induced biofilm calcification and calcium concentrations in phanerozoic oceans. *Science* **292,** 1701–1704.

Archer D. and Maier-Reimer E. (1994) Effect of deep-sea sedimentary calcite preservation on atmospheric CO2 concentrations. *Nature* **367,** 260–263.

Barker S. and Elderfield H. (2002) Foraminiferal calcification response to glacial-interglacial changes in atmospheric CO2. *Science* **297,** 833–836.

Ben-Yaakov S. and Goldhaber M. B. (1973) The influence of seawater composition on the apparent constants of the carbonate system. *Deep-Sea Research* **20,** 87–99.

Berner R. A., Lasaga A. C., and Garrels R. M. (1983) The carbonate-silicate geochemical cycle and its effect on atmospheric carbon dioxide over the past 100 million years. *Am. J. Sci.* **283,** 641–683.

Berner R. A. (1994) 3GEOCARB II: a revised model of atmospheric CO2 over phanerozoic time. *Am. J. Sci.* **294,** 56–91.

Berner E. K. and Berner R. A. (1996) *Global Environment: Water, Air, and Geochemical Cycles*. Prentice Hall.

Berner R. A. and Kothavala Z. (2001) GEOCARB III: A revised model of atmospheric CO2 over phanerozoic time. *American J. of Science* **301,** 182–204.

Broecker W. S. (1982) Ocean chemistry during glacial times. *Geochim. Cosmochim. Acta* **46,** 1689–1705.

Broecker W. S. and Peng T.-H. (1982) *Tracers in the Sea*. Lamont-Doherty Earth Observatory.

Broecker W. S. and Peng T.-H. (1998) *Greenhouse Puzzles (III): Walker's World*. (2nd edition), Eldigio Press.

Caldeira K. and Berner R. A. (1999) Seawater pH and atmospheric carbon dioxide. *Science* **286,** 2043a.

Demicco R. V., Lowenstein T. K., and Hardie L. A. (2003) Atmospheric pCO2 since 60 Ma from records of seawater pH, calcium, and primary carbonate mineralogy. *Geol.* **31,** 793–796.

Dickson J. A. D. (2002) Fossil echinoderms as monitor of the Mg/Ca ratio of phanerozoic oceans. *Science* **298,** 1222–1224.

Flower B. P. (1999) Palaeoclimatology: Warming without high CO_2? *Nature* **399,** 313–314.

Hardie L. A. (1996) Secular variation in seawater chemistry: An explanation for the coupled secular variation in the mineralogies of marine limestones and potash evaporites over the past 600 my. *Geol.* **24,** 279–283.

Harvey L. D. D. (2001) A quasi-one-dimensional coupled climate-carbon cycle model 2. The carbon cycle component. *J. of Geophysical Research-Oceans* **106,** 22355–22372.

Hay W. W. (1988) Paleoceanography: a review for the GSA centennial. *Geol. Soc. Amer. Bull.* **100,** 1934–1956.

Hay W. W. (1999) Carbonate sedimentation through the late Precambrian and Phanerozoic. *Zbl. Geol. Palaont. Teil I* **5–6,** 435–445.

Hay W. W., Wold C. N., Soding E., and Flogel S. (2001) Evolution of sediment fluxes and ocean salinity. In *Geologic Modeling and Simulation: Sedimentary Systems* (ed. D. F. Merriam and J. C. Davis), pp. 153–167, Kluwer Academic.

Holland H. D. (1978) *The Chemistry of the Atmosphere and the Oceans*. Wiley.

Holland H. D. (1984) *The Chemical Evolution of the Atmosphere and Ocean*. Princeton University Press.

Holland H. D. and Zimmermann H. (1998) On the secular variations in the composition of Phanerozoic marine potash evaporites: Reply. *Geol.* **26,** 92–92.

Holland H. D. and Zimmerman H. (2000) The dolomite problem revisited. *International Geology Review* **42,** 481–490.

Holland H. D., Horita J., and Seyfried W. E. (1996) On the secular variations in the composition of Phanerozoic marine potash evaporites. *Geol.* **24,** 993–996.

Horita J., Zimmermann H., and Holland H. D. (2002) Chemical evolution of seawater during the Phanerozoic: Implications from the record of marine evaporites. *Geochim. Cosmochim. Acta* **66,** 3733–3756.

Jansen H., Zeebe R. E., and Wolf-Gladrow D. A. (2002) Modeling the dissolution of settling CaCO3 in the ocean. *Global Biogeochemical Cycles* **16,** art. no.-1027.

Kump L. R. and Arthur M. A. (1997) Global chemical erosion during the Cenozoic: weatherability balances the budgets. In *Tectonic Uplift and Climate* (ed. W. F. Ruddiman), pp. 399–426. Plenum Press.

Lear C. H., Rosenthal Y., and Slowey N. (2002) Benthic foraminiferal Mg/Ca-paleothermometry: A revised core-top calibration. *Geochim. Cosmochim. Acta* **66,** 3375–3387.

Lemarchand D., Gaillardet J., Lewin E., and Allegre C. J. (2000) The influence of rivers on marine boron isotopes and implications for reconstructing past ocean pH. *Nature* **408,** 951–954.

Lowenstein T. K., Timofeeff M. N., Brennan S. T., Hardie L. A., and Demicco R. V. (2001) Oscillations in Phanerozoic seawater chemistry: Evidence from fluid inclusions. *Science* **294,** 1086–1088.

Lueker T. J., Dickson A. G., and Keeling C. D. (2000) Ocean pCO(2) calculated from dissolved inorganic carbon, alkalinity, and equations for K-1 and K-2: validation based on laboratory measurements of CO2 in gas and seawater at equilibrium. *Marine Chemistry* **70,** 105–119.

Lyle M. (2003) Neogene carbonate burial in the Pacific Ocean. *Paleoceanography* **18,** doi:10.1029/2002PA000777.

Millero F. J. and Schreiber D. R. (1982) Use of the Ion-Pairing Model to Estimate Activity-Coefficients of the Ionic Components of Natural-Waters. *American J. of Science* **282,** 1508–1540.

Montanez I. P. (2002) Biological skeletal carbonate records changes in major-ion chemistry of paleo-oceans. *Proceedings of the National Academy of Sciences of the United States of America* **99,** 15852–15854.

Morse J. W., Wang Q. W., and Tsio M. Y. (1997) Influences of temperature and Mg: Ca ratio on CaCO3 precipitates from seawater. *Geol.* **25,** 85–87.

Mucci A. (1983) The solubility of calcite and aragonite in seawater at various salinities, temperatures, and one atmosphere total pressure. *American J. of Science* **283,** 780–799.

Mucci A. and Morse J. W. (1984) The solubility of calcite in seawater solutions of various magnesium concentration, It=0.697-M at 25-degrees-C and one atmosphere total pressure. *Geochim. Cosmochim. Acta* **48,** 815–822.

Opdyke B. N. and Wilkinson B. H. (1989) Surface area control of shallow cratonic to deep marine carbonate accumulation. *Paleoceanography* **3,** 685–703.

Opdyke B. N. and Wilkinson B. H. (1990) Paleolatitude distribution of phanerozoic marine ooids and cements. *Palaeogeography Palaeoclimatology Palaeoecology* **78,** 135–148.

Opdyke B. N. and Wilkinson B. H. (1993) Carbonate mineral saturation state and cratonic limestone accumulation. *American J. of Science* **293,** 217–234.

Pagani M., Arthur M. A., and Freeman K. H. (1999) Miocene evolution of atmospheric carbon dioxide. *Paleoceanography* **14,** 273–292.

Pearson P. N. and Palmer M. R. (1999) Middle Eocene seawater pH and atmospheric CO2 concentrations. *Science* **284,** 1824–1826.

Pearson P. N. and Palmer M. R. (2000) Atmospheric carbon dioxide concentrations over the past 60 million years. *Nature* **406,** 695–699.

Peterson L. C. and Backman J. (1990) Late Cenozoic carbonate accumulation and the history of the carbonate compensation depth in the western equatorial Indian Ocean. *Proceedings of the Ocean Drilling Program, Scientific Results.* **115,** 467–489.

Prieto F. J. M. and Millero F. J. (2002) The values of pK(1)+ pK(2) for the dissociation of carbonic acid in seawater. *Geochim. Cosmochim. Acta* **66,** 2529–2540.

Royer D. L., Wing S. L., Beerling D. J., Jolley D. W., Koch P. L., Hickey L. J., and Berner R. A. (2001) Paleobotanical evidence for near present-day levels of atmospheric CO2 during part of the tertiary. *Science* **292,** 2310–2313.

Sandberg P. A. (1983) An oscillating trend in phanerozoic non-skeletal carbonate mineralogy. *Nature* **305,** 19–22.

Sarmiento J. L., Dunne J., Gnanadesikan A., Key R. M., Matsumoto K., and Slater R. (2002) A new estimate of the CaCO3 to organic carbon export ratio. *Global Biogeochemical Cycles* **16,** art. no.1107.

Sclater J. G., Abbott D., and Thiede J. (1977) Paleobathymetry and sediments of the Indian Ocean. In *Indian Ocean Geology and Biostratigraphy* (eds. J. R. Heirtzler et al.), pp. 25–60. American Geophysical Union.

Sigman D. M., McCorkle D. C., and Martin W. R. (1998) The calcite lysocline as a constraint on glacial/interglacial low-latitude production changes. *Global Biogeochemical Cycles* **12,** 409–427.

Spencer R. J. and Hardie L. A. (1990) Control of seawater composition by mixing of river waters and mid ocean ridge hydrothermal bines. In *Fluid-mineral interactions: A tribute to H.P. Eugster* (ed. R. J. Spencer and I.-M. Chou), pp. 409–412. Geochemical Society Special Publication, No. 2.

Stanley S. M. and Hardie L. A. (1998) Secular oscillations in the carbonate mineralogy of reef- building and sediment-producing organisms driven by tectonically forced shifts in seawater chemistry. *Palaeogeography Palaeoclimatology Palaeoecology* **144,** 3–19.

Stanley S. M., Ries J. B., and Hardie L. A. (2002) Low-magnesium calcite produced by coralline algae in seawater of Late Cretaceous composition. *Proceedings of the National Academy of Sciences of the United States of America* **99,** 15323–15326.

Sundquist E. T. (1990) Influence of deep-sea benthic processes on atmospheric CO2. *Philosophical Transactions of the Royal Society of London Series a-Mathematical Physical and Engineering Sciences* **331,** 155–165.

Sundquist E. T. (1999) Seawater pH and atmospheric carbon dioxide. *Science* **286,** 2043a.

Takahashi T. (1989) The carbon dioxide puzzle. *Oceanus* **32,** 22–29.

Thomas E. (1998) Biogeography of the late Palaeocene benthic foraminiferal extinction. In *Last Palaeocene-early Eocene climatic and biotic events* (ed. M.-P. Aubry et al.), pp. 214–243. Columbia University Press.

van Andel T. H. (1975) Mesozoic/Cenozoic calcite compensation depth and the global distribution of calcareous sediments. *Earth and Planetary Science Letters* **26,** 187–194.

Veizer J., Godderis Y., and Francois L. M. (2000) Evidence for decoupling of atmospheric CO2 and global climate during the Phanerozoic eon. *Nature* **408,** 698–701.

Volk T. (1989) Sensitivity of climate and atmospheric CO2 to deep-ocean and shallow-ocean carbonate burial. *Nature* **337,** 637–640.

Wilson P. A., Norris R. D., and Cooper M. J. (2002) Testing the Cretaceous greenhouse hypothesis using glassy foraminiferal calcite from the core of the Turonian tropics on Demerara Rise. *Geol.* **30,** 607–610.

Yamanaka Y. and Tajika E. (1996) The role of the vertical fluxes of particulate organic matter and calcite in the ocean carbon cycle: Studies using an ocean biogeochemical general circulation model. *Global Biogeochemical Cycles.* **10,** 361–382.

Zachos J., Pagani M., Sloan L., Thomas E., and Billups K. (2001) Trends, rhythms, and aberrations in global climate 65. Ma to present. *Science* **292,** 686–693.

Zeebe R. E. and Westbroek P. (2003) A simple model for the CaCO3 saturation state of the ocean: the "Strangelove," the "Neritan," and the "Cretan" ocean. *Geochemistry, Geophysics, Geosystems* **4,** doi: 10.1029/2003GC000538.

Zeebe R. E. and Wolf-Gladrow D. A. (2001) *CO2 in Seawater: Equilibrium, Kinetics, Isotopes*. Elsevier.

Zimmermann H. (2000) Tertiary seawater chemistry - Implications from primary fluid inclusions in marine halite. *American J. of Science* **300,** 723–767.

APPENDIX

In this appendix we consider the sensitivity of our results to uncertainties about past vertical gradients in the ocean. If the difference between surface and deep carbonate ion concentration ($\Delta[CO_3^{2-}]$) was very different in the past compared to today, then it is possible that while deep ocean saturation state stayed more or less constant (i.e., CCD between 3.5 and 5 km, as suggested by the data), at the same time surface ocean saturation state could have varied. For instance, $\Delta[CO_3^{2-}]$ could have changed because of variability in the organic and/or inorganic carbon pumps. In this study we assume near-constant surface ocean saturation state even though the CCD is a direct constraint only on deep saturation state. Some support for this assumption comes from the evidence summarised in section 1.4 (points B, C and D), and also from the long-term record of $\Delta\delta^{13}C$ (the difference between the $\delta^{13}C$ values recorded in planktic and benthic foraminifera). According to the summary by Broecker and Peng (1998), the surface-to-deep gradient in $\delta^{13}C$ has stayed rather constant over time. While this suggests that the organic carbon pump strength has not varied greatly, it does not constrain the past behaviour of the inorganic carbon pump.

Because of this uncertainty about past vertical gradients, we generate results for a range of different values and then analyse the results to determine: (i) which results agree with the $\Delta\delta^{13}C$ record, and also (ii) which results produce non-negative Δ[TA].

There are two degrees of freedom in both of the surface and the deep, four in all. We already know $[CO_3^{2-}]_d$ and either pH_s or $pCO2_s$, depending on the run, leaving two degrees of freedom. It is not possible to calculate unambiguously both the surface (subscript 's') and deep (subscript 'd') complete carbonate system chemistries by assuming values for Δ[DIC] and Δ[TA]. Our approach, therefore, is to vary

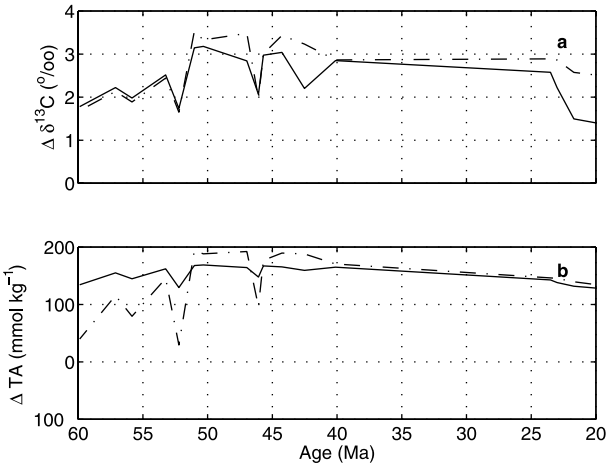

Fig. 6. Illustration of the sensitivity study. Calculated results for (a) surface-to-deep gradient of $\delta^{13}C$ of DIC ($\Delta\delta^{13}C$) and (b) surface-to-deep gradient in total alkalinity (ΔTA) for the standard run (solid lines, Δ[DIC] = 250 μmol kg^{-1} and $f = f_m$) and for Δ[DIC] = 200 μmol kg^{-1} and $f = f_m \times 1.25$ (dot-dashed lines). For the latter run, ΔTA becomes negative at ~52 My and parameter variations larger than that can be excluded (see text).

Table A.1.

Run #	f/f_m	Δ[DIC] (μmol kg^{-1})	pCO_2[a] (μatm)	$\Delta\delta^{13}C$[b] (‰)	ΔTA[b] (μmol kg^{-1})	Admissible
1	0.75	200	2470	0.3–3.0	~150	NO[c]
2	1.00	200	3290	1.0–2.5	~100	YES
3	1.25	200	4120	1.0–2.0	Negative	NO
4	0.75	250	2470	0.3–2.5	>200	NO[c]
5[d]	1.00	250	3290	1.5–3.0	~100–150	YES
6	1.25	250	4120	0.5–3.0	~100	NO[c]
7	0.75	300	2470	0.4–4.0	~200–250	NO
8	1.00	300	3290	1.5–3.5	~200	NO[c]
9	1.25	300	4120	2.0–3.0	~100–150	YES

YES = $\Delta\delta^{13}C$ and ΔTA admissible; NO = $\Delta\delta^{13}C$ or ΔTA not admissible.

[a] Value at 60 Ma (compare figure 3).

[b] Values between 20 and 60 Ma.

[c] Limit. A further change of f/f_m or Δ[DIC] is not admissible.

[d] Standard run, i.e. assuming modern f/f_m and Δ[DIC] (Figure 3).

instead Δ[DIC] and $[CO_3^{2-}]_s$. As in most sensitivity analyses, this choice is somewhat arbitrary. However, in the present case there is a reason for it. First, Δ[DIC] is mainly controlled by the organic carbon pump—recent estimates of the organic to carbonate rain ratio range from 10:1 to 17:1 (Yamanaka and Tajika, 1996; Harvey, 2001; Sarmiento et al., 2002). As a result, variations of Δ[DIC] in our sensitivity analysis directly cause variations of $\Delta\delta^{13}C$ that can be checked against data. Second, varying $[CO_3^{2-}]_s$ makes sense as it is directly related to the $CaCO_3$ saturation state which was assumed nearly constant in the deep—as well as in the surface ocean. For the sensitivity analysis, we use:

$$[DIC]_d = [DIC]_s + \Delta[DIC] \quad (2)$$

$$[CO_3^{2-}]_s = f \times [CO_3^{2-}]_d \quad (3)$$

where Δ[DIC] and f will be varied. The mathematical form of (2) is a consequence of the nature of the organic pump which produces an offset between surface and deep ocean. The form of (3)—which implies a proportionality between surface and deep $[CO_3^{2-}]$—is justified as follows. The evidence summarised in section 1.4 argues against dramatic changes of the saturation state of both surface and deep ocean over time. Using Eqn. 1, this requires that the ratio of $[CO_3^{2-}]_s/[CO_3^{2-}]_d$ must have been approximately constant from which Eqn. 3 follows.

Using the approach described above, $[CO_3^{2-}]_s$ can then be calculated from Eqn. 3, because $[CO_3^{2-}]_d$ is known initially—allowing the whole surface carbonate chemistry to be worked out, including $[DIC]_s$. $[DIC]_d$ is then calculated from Eqn. 2.

Δ[DIC] in the modern ocean is equal to ~250 μmol kg^{-1} (deep value of ~2250 μmol kg^{-1}, surface average value of ~2000 μmol kg^{-1}; Takahashi, 1989), and modern f ($=f_m$) to ~2.2 (deep value of $[CO_3^{2-}]$~90 μmol kg^{-1}, surface average value of ~200 μmol kg^{-1}). The carbonate ion concentrations were calculated using DIC as given above and TA = 2370 μmol kg^{-1}, T = 4°C, S = 35, P = 300 atm (deep), and at TA = 2300 μmol kg^{-1}, T = 15°C, S = 35, P = 1 atm (surface).

The values for $\Delta\delta^{13}C$ were calculated according to (Broecker, 1982):

$$\Delta\delta^{13}C = -(\Delta^{photo}) \times \Delta[DIC]/[DIC]_{mean} \quad (4)$$

where Δ^{photo} is a photosynthetic fractionation factor and $[DIC]_{mean}$ is the mean DIC of the ocean. The effect of [CO2(aq)] on Δ^{photo} was taken into account by:

$$\Delta^{photo} = a + b/[CO_2(aq)] \quad (5)$$

using $b = 117 \times 10^{-6}$ (Pagani et al., 1999) and $a = -29$ to match the modern $\Delta\delta^{13}C$ of ~2‰.

The sensitivity of the model results are now evaluated as follows. Model calculations for the carbonate chemistry over the last 60 My (cf. Fig. 3) are carried out, including calculations for $\Delta\delta^{13}C$ and ΔTA (Fig.

6 and Table A.1). Model results for all combinations of Δ[DIC] = {200, 250, 300} μmol kg^{-1} and $f = f_m \times$ {0.75, 1.00, 1.25}, i.e., a total of $3 \times 3 = 9$ runs were obtained. Figure 6 shows the results for the standard run (solid lines, Δ[DIC] = 250 μmol kg^{-1} and $f = f_m$) and for Δ[DIC] = 200 μmol kg^{-1} and $f = f_m \times 1.25$ (dot-dashed lines). In the latter simulation, ΔTA becomes negative at $\sim$52 My and hence this solution is discarded because it would mean that the carbonate pump must have worked in the opposite direction to reverse the alkalinity gradient.

After we discard all solutions with negative ΔTA or $\Delta\delta^{13}$C values at odds with the data ($\Delta\delta^{13}C < 1$ or $\Delta\delta^{13}C > 3$), then we are left with model runs #2, #5, and #9 that yield reasonable results (Table A.1). Run #5 is our standard run, i.e., assuming the modern relationship between surface and deep [CO_3^{2-}] ($f/f_m = 1$) and Δ[DIC] = 250 μmol kg^{-1} for the past (compare Fig. 3). Run #2 and #9 suggest that a further change of parameters may still lead to reasonable results. For run #2, a further decrease of Δ[DIC] is still possible but does not lead to a change of pCO_2 because surface pH and [CO_3^{2-}] are already set by the data and $f/f_m = 1$. For run #9, a further parallel increase of the two parameters appears reasonable up to $f/fm = 1.5$ and Δ[DIC] = 350 μmol kg^{-1}. This suggests an upper limit of pCO_2 values of $\sim$4900 μatm at 60 My for the reconstruction based on our [CO_3^{2-}] and the pH values from Pearson and Palmer (2000).

In summary, the sensitivity study shows that: (i) our initial assumption of similar past and modern surface-to-deep gradients is reasonable and neither violates observational constraints on $\Delta\delta^{13}$C nor leads to unrealistic or negative ΔTA; and (ii) the limits obtained from our analysis suggest an uncertainty of ca. $\pm$25% in calculated [CO_3^{2-}]$_s$ (being proportional to f/f_m) and ca. $\pm$25% in pCO_2 values due to variations in surface-to-deep gradients. If both surface saturation state ([CO_3^{2-}]$_s$) and Δ[DIC] were larger in the past, then the upper limit of uncertainty as suggested by our analysis is about +50% in pCO_2. Note, however, that large changes in [CO_3^{2-}]$_s$ would conflict with the evidence summarised in Section 1.4 (points B, C and D).